# Phaseless antenna diagnostics based on off-axis holography with synthetic reference wave

Jaime Laviada, Ana Arboleya-Arboleya, *Student Member, IEEE*, Yuri Álvarez-López, *Member, IEEE*, Cebrián García-González, *Student Member, IEEE*, and Fernando Las-Heras, *Senior Member, IEEE*

***Abstract*—An antenna diagnostics method based on off-axis holography is presented in this paper. In this novel phaseless antenna measurement setup, the reference wave is synthesized by means of a mechanical phase shifting and, therefore, the use of a phase shifter is avoided, yielding an accurate low-cost antenna diagnostics system. The technique is validated by means of simulation as well as measurement. Accurate results prove the system capability for antenna diagnostics tasks.**

## I. Introduction

Antenna diagnostics involves the detection of failures which prevent the antenna from achieving its ideal performance. The identification and correction of antenna design and manufacturing errors usually requires invasive techniques based on trial-error procedure whose technical and economical costs are directly related to the antenna complexity. Thus, the development of fast and accurate non-invasive methods for antenna faults detection has been of great interest in the last decade.

Non-invasive methods are usually based on acquiring the antenna radiated field and, after that, computing a set of key parameters such as the extremely near-field on the antenna aperture [1] or the equivalent currents on the antenna surface [2], [3]. Antenna manufacturing errors can be easily detected from the analysis of these parameters. For example, any distortion on the reflector antenna surface appears as a phaseshift in the retrieved near-field on the antenna aperture [1].

The computation of these parameters involves, in general, the acquisition of the amplitude and phase of the field. Although the amplitude acquisition is relatively simple at any frequency, the phase acquisition can be complex at high frequencies or in environments with poor thermal stability [4], [5].

In order to accomplish a succesful diagnostics from amplitude-only measurements, several phase retrieval techniques for radiated fields are available in the literature. Many of them rely on iterative schemes (e.g., [6], [7]) relating the fields (or equivalent currents) in two (or more) different surfaces.

The authors are with the department of Electrical Engineering\\ Universidad de Oviedo\\ Campus Universitario, 33203 Gijón, Asturias, Spain\\ Authors' email: {jlaviada, aarboleya, yalopez, cgarciag, flasheras }@tsc.uniovi.es

This work has been supported supported in part by the European Union under COST Action IC1102 (VISTA); by the Ministerio de Ciencia e Innovación of Spain /FEDER under projects TEC2011- 24492 (iScatt), CSD2008-00068 (Terasense) and MICINN-11-IPT-2011-0951-390000 (Tecnigraf); by the Gobierno del Principado de Asturias (PCTI)/FEDER-FSE under projects PC10-06, EQUIP08-06, FC09-C0F09-12, EQUIP10-31; by grants BP-11-169 of the Gobierno del Principado de Asturias and BES-2009-024060.

On the other hand, iteration-free phase retrieval can be accomplished by means of the Leith-Upatnieks holography [8] if a conveniently characterized source is included in the setup. This source can be replaced by a synthesized reference wave which enables a total control of the system (see [9] and the references therein). Despite of the flexibility of this setup, it involves the use of digital phase shifters which can considerably increase the cost of the overall setup at high frequencies.

In this letter, the Leith–Upatnieks approach is applied to the antenna diagnostics by synthesizing the reference wave through the mechanical displacement of the probe antenna. Thus, the inverse scattering scheme in [10] is reformulated in order to apply it to fault antenna measurements. It results in a simplified, low-cost scheme that can be used to carry out accurate antenna diagnostics.

## II. Antenna diagnostics via enhanced Leith-Upatnieks holography

### A. Setup for the phase retrieval

In the Leith-Upatnieks holography, the field from the antenna under test (AUT) is combined with a reference field, whose amplitude and phase are known on the acquisition surface, yielding the following received hologram:

$$I(\vec{r}) = \left| E_{AUT}\left(\vec{r}\right) + E_r\left(\vec{r}\right) \right|^2, \tag{1}$$

wherein $E_{AUT}$ is the field radiated by the antenna under test and $E_r$ is the field of the reference antenna. Multiple setups have been proposed in the literature to implement this interferometry scheme (e.g., [5]). A conventional assumption is to approximate the reference field by a plane wave so $E_r\left(r'\right) = A\exp(-jk_0\hat{k}\cdot r')$ being $k_0$ the free space wavenumber and $\hat{k}$ the unitary propagation vector of the plane wave.

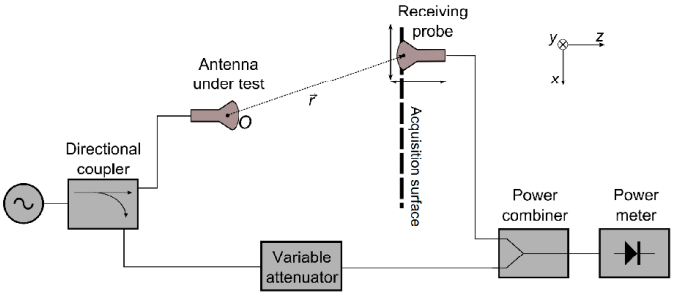


Figure 1. Setup for the phaseless diagnostics based on Leith-Upatnieks holography.

Next, it will be shown that the setup in Fig. 1, which does not employ a phase shifter as conventional schemes [11], [12], can enable an acquisition equivalent to the one in (1). In this scheme, the field received at the probe antenna located at the acquisition point defined by $\vec{r}$ is given by:

$$I(\vec{r}) = \left|E_{AUT}(\vec{r}) + C\right|^2, \tag{2}$$

wherein $C$ is the constant signal injected though the variable attenuator branch. This variable attenuator is used to balance the power between the two branches arriving to the power combiner. Its value is only tuned at the beginning of the measurement so that the amplitude of the constant signal matches approximately the value of the field due to the AUT.

If the probe antenna is displaced a distance $\vec{d} = d\frac{\vec{r}}{\|\vec{r}\|_2}$, then the field at the modified acquisition point $\vec{r}\,' = \vec{r} + \vec{d}$ is given by:

$$E_{AUT}(\vec{r}\,') \approx E_{AUT}(\vec{r}) e^{-jk_0 d}. \tag{3}$$

Thus, the received hologram at the modified point is given by:

$$I(\vec{r}\,') \approx \left|E_{AUT}(\vec{r})\, e^{-jk_0 d} + C\right|^2 = \left|E_{AUT}(\vec{r}) + Ce^{jk_0 d}\right|^2. \tag{4}$$

Eq. (4) shows that if the appropriate displacement is chosen for each original point, then sampling in the modified points results in the same acquired hologram as in the case of using the conventional acquisition points together with an interfering plane-wave. As a consequence, the use of a phase shifter, which can be complex and expensive at high frequencies, is replaced by a three dimensional movement that can be carried out with micropositioners.

It is important to note that the approximation in (3) is only valid if the probe is in the far-field of the antenna. However, in the results section, it will be shown that this approximation can provide accurate results for diagnostics purposes although this condition is not strictly fulfilled. The reason is that the maximum displacement is $d = \pm\lambda/2$, which results in a phase shift of $\pm 180°$. These electrically small movements make possible to assume that the amplitude remains unchanged whereas the phase is linearly modified.

### *B. Postprocessing algorithm*

In the indirect holography, two different postprocessing techniques are possible depending on the sampling rate. In order to understand the one that is used in this letter, let us consider the spectrum of the acquired hologram which is given by the Fourier transform of (1). In this section, it is assumed that phase shifting is applied along the $x$-axis without loss of generality. The wavenumber of the synthesized plane-wave is denoted by $k_x^{pw}$; then, the received hologram is given by:

$$\begin{aligned} I(x,y) &= \left|E_{AUT}(x,y) + Ce^{-jk_x^{pw}x}\right|^2 \\ &= |C|^2 + |E_{AUT}(x,y)|^2 \\ &+ C^* E_{AUT}(x,y)\, e^{jk_x^{pw}x} + CE^*_{AUT}(x,y)\, e^{-jk_x^{pw}x}. \end{aligned} \tag{5}$$

The spectrum of the received hologram is calculated by means of the Fourier transform of the previous expression and it is shown in Fig. 2. In this figure, the tilde is used to denote Fourier transform and $W$ is the bandwidth of the radiated field.

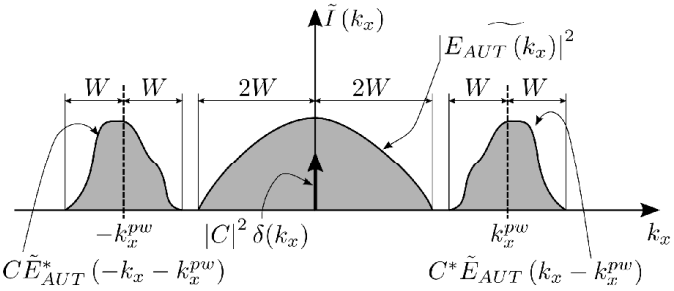


Figure 2. Spectrum of the acquired hologram.

Four terms can be identified in the spectrum. The first term corresponds to a Dirac delta function which is at the origin of the spectral axis. In addition, a second term, which corresponds to the Fourier transform of the squared amplitude of the field, is also centered at the origin of the spectral axis. The bandwidth of this term is twice the bandwidth of the radiated field $E_{AUT}$. The two remaining terms are centered at $\pm k_x^{pw}$and correspond to the spectrum of the radiated field as well as the spectrum of its complex conjugate. Thus, if one of these two terms is isolated, then the spectrum (and so the amplitude and phase) of the radiated field can be retrieved.

According to [13], the spatial bandwidth of the radiated field for planar acquisition can be consider as $W = k_0$ in the region of interest. Hence, the wavenumber of the equivalent plane wave must be at least $k_x^{pw} = 3k_0$ to avoid spectral overlapping.

The conventional way to implement the phase shifting along a given direction is to use a constant increment of the phase of the reference wave $\Delta\phi$ between consecutive samples. Under this assumption, the wave number of the equivalent plane wave is given by $k_x^{pw} = \frac{\Delta\phi}{\Delta x}$ [12], wherein $\Delta x$ is the sampling step. Since the total bandwidth of the signal is $4W = 4k_0$, then the sampling step must be at least $\Delta x = \lambda/8$. According to this step size, the optimal phase increment is given by $\Delta\phi = 135°$.

Another possible way to retrieve the amplitude and phase is to use the so-called *modified hologram*. This hologram is computed by subtracting the squared amplitude of the reference and radiated field from the acquired hologram. By doing this, the two central terms in the Fig. 2 are removed. As a consequence, the two remaining spectra, which corresponds to the radiated field and its complex conjugate, can get closer. In particular, the optimal value of the wavenumber of the equivalent plane-wave is now given by $k_x^{pw} = k_0$. Thus, the total bandwidth of the modified hologram is $2W = 2k_0$ yielding a minimum sampling step size of $\Delta x = \lambda/4$. Thus, the optimal phase increment is given by $\Delta\phi = 90°$ in case of considering the modified hologram.

Although the use of the modified hologram requires a lower sampling rate, it involves a double acquisition in order to compute the hologram and the amplitude of the radiated field. Thus, the acquisition environment must be stable along both acquisitions. On the other hand, the direct processing of the received hologram involves a single acquisition (with the double of points).

In this work, a trade-off between both possibilities has been applied. Thus, the acquired hologram is directly processed without computing the modified hologram so that the need of two consecutive acquisitions is avoided. However, the phase shift and sampling rate are fixed to $\Delta\phi = 90^\circ$ and $\Delta x = \lambda/8$. The reason for this choice is that the equivalent wavenumber $k_x^{pw} = 2k_0$ and the maximum acquired spectral frequency $\frac{\pi}{\Delta x} = 4k_0$ enables centering the spectra. Although this set of parameter values results in certain overlapping with the central terms, it will be shown in the results section that it has not a significant impact in the final solution. The reason is that, although the spectrum of the central term corresponding to the square amplitude has a bandwidth of $2k_0$, this spectrum decays very quickly in practice as it comes from the convolution between two spectra which are expected to vanish at $k_0$. Thus, a certain degree of overlapping can be tolerated without significantly degrading the performance of the technique.

## III. Antenna Diagnostics Examples

In this section, simulations and measurements are carried out to validate the performance of the proposed technique for antenna diagnostics purposes. In the case of simulation-based example (subsection III-A), the antenna is simulated and the radiated field is acquired in the modified points. After that, a constant signal is added and the squared amplitude of the resulting signal is processed to retrieve the amplitude and phase of $E_{AUT}$.

Concerning the measurement example (subsection III-B), the combined signal is acquired with a vector network analyzer (VNA) and, after that, the squared amplitude is postprocessed. Thus, no phase information is used at any point.

### A. Simulated patch array

In this example, a two dimensional array of rectangular patches, as shown in Fig. 3, is considered. The elements are placed on a substrate with electrical permittivity $\epsilon_r = 2.2$ and thickness $h = 2.87\,\text{mm}$ with uniform amplitude and phase feeding. The working frequency is $3\,\text{GHz}$. The method of moments is used to simulate this array. Green's function for multilayered planar substrates is used and, consequently, the substrate and ground plane are considered as infinite.

The acquisition surface, which is two meters over the patch array plane, is a square plane of edge equals to $5\,\text{m}$. The phase shifting is applied along the $x$-axis with a phase increment $\Delta\phi = 90^\circ$. The sampling steps for each direction are $\Delta x = \lambda/8$ and $\Delta y = \lambda/2$.

In order to check the accuracy of the method, the following error is computed:

$$e[\%] = \frac{\|\mathbf{E}_{ret} - \mathbf{E}_{ref}\|_2}{\|\mathbf{E}_{ref}\|_2} \cdot 100, \qquad (6)$$

wherein $\mathbf{E}_{ret}$ is a vector containing the samples of the field radiated by the antenna retrieved at the acquisition points whereas $\mathbf{E}_{ref}$ is a vector containing the samples of the field directly computed by means of the method of moment. In this analysis, only the main component of the field is considered ($y$-component).

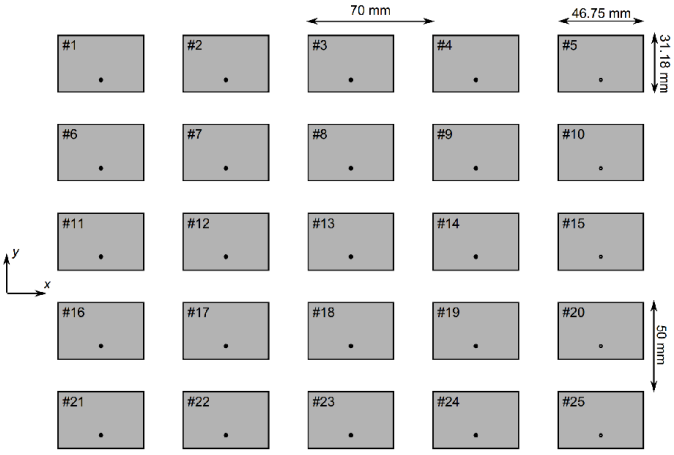


Figure 3. Array of rectangular patches. Dots near the lower edge of each patch represent the feeding point.

A failure in the element #12 is considered next. This failure is modeled by zero feeding of this element. The total error in this case is 2.15% and, therefore, accurate results can be expected for diagnostics purposes. After backpropagating the retrieved field to the antenna aperture [14], the fault element can be clearly identified as shown in Fig. 4a. The robustness of the algorithm in case of noisy environments is also considered. Thus, Fig. 4b corresponds to the field backpropagated to the aperture in the case of a signal to noise ratio equal 10 dB. Despite of the strong noise, the backpropagated field is still accurate enough to identify the fault element. Thus, the effect of the noise is not expected to spoil the performance of the phase retrieval algorithm for diagnostics purposes.

### B. Obstacle in front of a horn antenna

A horn antenna with an obstacle between the antenna and the acquisition surface is considered in this example. The working frequency is fixed at 30 GHz.

The dimensions of the acquisition surface, which is placed at 20 cm from the aperture plane, are $40\,\text{cm} \times 34\,\text{cm}$. An 'U'-shaped obstacle is placed at 5 cm from the horn in order to check if it can be detected. Foam is used to hold the obstacle over the antenna so minor perturbations are expected due to the supporting structure.

After retrieving the amplitude and phase, the field was back-propagated to multiple planes [14] in order to find the position and shape of the obstacle. Fig. 6 shows the backpropagated field in the plane at 15 cm wherein the U-shaped object can be clearly detected.

## IV. Conclusions

An indirect holography scheme for antenna diagnostics applications has been presented. In the implemented setup, the reference wave has been synthesized by means of a mechanical displacement of the probe. Thus, plane waves beyond the visible spectrum can be synthesized without requiring a phase shifter.

The optimal phase shifting and sampling rates have also been discussed on theoretical basis. A trade-off solution has

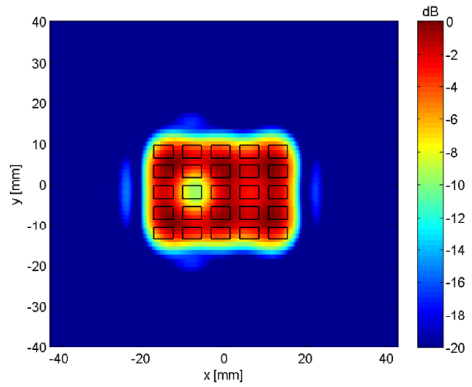


(a) SNR=∞

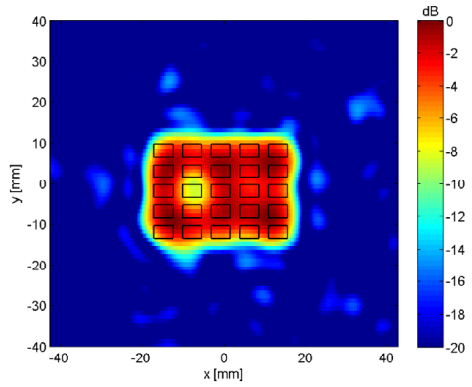


(b) SNR=10 dB

Figure 4. Normalized retrieved field distribution in the aperture of the patch array antenna.

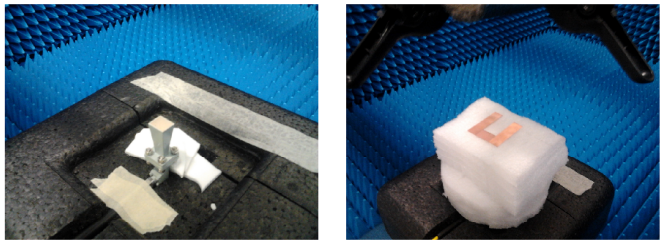

(a) (b)

Figure 5. Measurement setup for the horn antenna with obstacle: a) antenna without any obstacle; b) antenna with a 'U' obstacle.

been proposed by considering a non-significant overlapping between some spectral terms.

Although the mechanical phase shifting is based on a far-field approximation, numerical simulations have shown that the final error is low enough to enable successful application in antenna diagnostics methods. The presented results from amplitude-only measurements confirm the validity of the proposed scheme for antenna diagnostics.

## REFERENCES

[1] Y. Álvarez, C. Cappellin, F. Las-Heras, and O. Breinbjerg, "On the comparsion of the spherical wave expansion-to-plane wave expansion and the sources reconstruction method for antenna diagnostics," *Progress In Electromagnetics Research*, vol. 87, pp. 245–262, 2008.

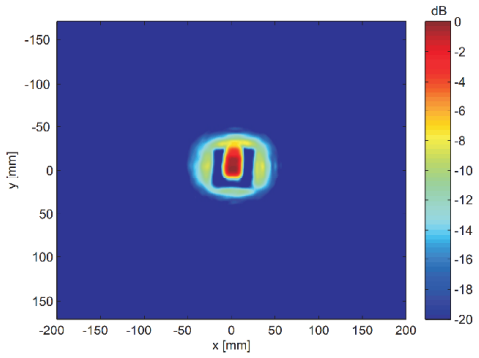


Figure 6. Field backpropagated for horn antenna with a 'U'-shaped obstacle.

[2] Y. Alvarez, F. Las-Heras, and M. Pino, "Reconstruction of equivalent currents distribution over arbitrary three-dimensional surfaces based on integral equation algorithms," *IEEE Trans. Antennas Propagat.*, vol. 55, no. 12, pp. 3460 –3468, Dec. 2007.

[3] J. Araque and G. Vecchi, "Field and source equivalence in source reconstruction on 3D surfaces," *Progress In Electromagnetics Research*, vol. 103, pp. 67–100, 2010.

[4] G. Hislop, L. Li, and A. Hellicar, "Phase retrieval for millimeter- and submillimeter-wave imaging," *IEEE Trans. Antennas Propagat.*, vol. 57, no. 1, pp. 286–289, Jan. 2009.

[5] G. Junkin, T. Huang, and J. Bennett, "Holographic testing of terahertz antennas," *IEEE Trans. Antennas Propagat.*, vol. 48, no. 3, pp. 409 –417, Mar. 2000.

[6] Y. Alvarez, F. Las-Heras, and M. R. Pino, "The sources reconstruction method for amplitude-only measurements," *IEEE Trans. Antennas Propagat.*, vol. 58, no. 8, pp. 2776–2781, Aug. 2010.

[7] P. Li and L. Jiang, "An iterative source reconstruction method exploiting phaseless electric field data," *Progress In Electromagnetics Research*, vol. 134, pp. 419–435, 2013.

[8] E. N. Leith and J. Upatnieks, "Reconstructed wavefronts and communication theory," *J. Opt. Soc. Amer.*, vol. 52, pp. 1123–1128, 1962.

[9] J. Laviada and F. Las-Heras, "Phaseless antenna measurement on non-redundant sample points via Leith-Upatnieks holography," *IEEE Trans. Antennas Propagat.*, vol. 61, no. 8, pp. 4036–4044, Aug. 2013.

[10] J. Laviada, Y. Álvarez López, C. García-González, A. Arboleya, and F. Las-Heras, "A modified phaseless inverse scattering setup based on indirect holography implemented at submillimeter-wave band," *IEEE Trans. Antennas Propagat.*, vol. 61, no. 9, pp. 4876–4881, Sep. 2013.

[11] V. Schejbal, V. Kovarik, and D. Cermak, "Synthesized-reference-wave holography for determining antenna radiation characteristics," *IEEE Antennas Propagat. Mag.*, vol. 50, no. 5, pp. 71 – 83, Oct. 2008.

[12] D. Smith, M. Leach, M. Elsdon, and S. J. Foti, "Indirect holographic techniques for determining antenna radiation characteristics and imaging aperture fields," *IEEE Antennas Propagat. Mag.*, vol. 49, no. 1, pp. 54 –67, Feb. 2007.

[13] A. Yaghjian, "An overview of near-field antenna measurements," *IEEE Trans. Antennas Propagat.*, vol. 56, no. 1, pp. 30–45, Jan. 1986.

[14] J. Hanfling, G. Borgiotti, and L. Kaplan, "The backward transform of the near field for reconstruction of aperture fields," in *Antennas and Propagation Society International Symposium, 1979*, vol. 17, 1979, pp. 764–767.